Electronic Supplementary Material (ESI) for Soft Matter.

SUPLEMENTARY INFORMATION

Acoustic Suppression of the Coffee-Ring Effect

Dileep Mampallil[1], Julien Reboud[1], Rab Wilson[1], Douglas Wylie[2], David Klug[2], Jonathan M. Cooper[1,*]

1. *Division of Biomedical Engineering, University of Glasgow, Oakfield Avenue, Glasgow, UK, G12 8LT. Email: jon.cooper@glasgow.ac.uk; Fax: +44 141-330 4907; Tel: +44 1413305231*
2. *Institute of Chemical Biology, Imperial College London, South Kensington, SW7 2AZ, London, UK*

Experimental methods

Preparation of the IDT. The IDT device was fabricated as described previously [1, 2], employing standard photolithography. The device consisted of gold interdigitated electrodes, with a pitch d=350 µm, and width w=175 µm on a 128° Y-cut X-propagating 3 inch $LiNbO_3$ wafer, patterned using lift-off process. The aperture of the device was 20 mm. The resonance frequency of the IDT depends on the separation between two adjacent electrode fingers, d and the sound velocity on the $LiNbO_3$ wafer, c=3990 m/s. The frequency is given as $f = c/(d/2)$. The frequencies generated by the IDT were characterized using a series network analyzer (Agilent Technologies E5071C ENA).

Preparation of the superstrate. We used glass, gold and steel surfaces as the superstrates. Standard microscope glass slides with thickness 1 mm were used in most of the experiments, unless otherwise specified. When indicated in the text, glass slides were treated in oxygen plasma for 10 seconds at 50 W power to make them more hydrophilic (resulting in an equilibrium contact angle of 12+/-2°). The Au surfaces were made by coating 100 nm gold layer by evaporation on 0.5 mm thick < 100 > Si wafer. A 20 nm Ti layer was deposited beforehand for adhesion. Superstrates were diced in 25 mm x 25 mm pieces. MALDI target plates were used as the steel superstrate. The superstrates were washed in acetone, ethanol, rinsed in deionized water and blow-dried with nitrogen before the measurements. The superstrates were characterized by measuring the contact angle and the contact angle hysteresis of water (EasyDrop, KRUSS GmBH, Germany) (see Fig. S1).

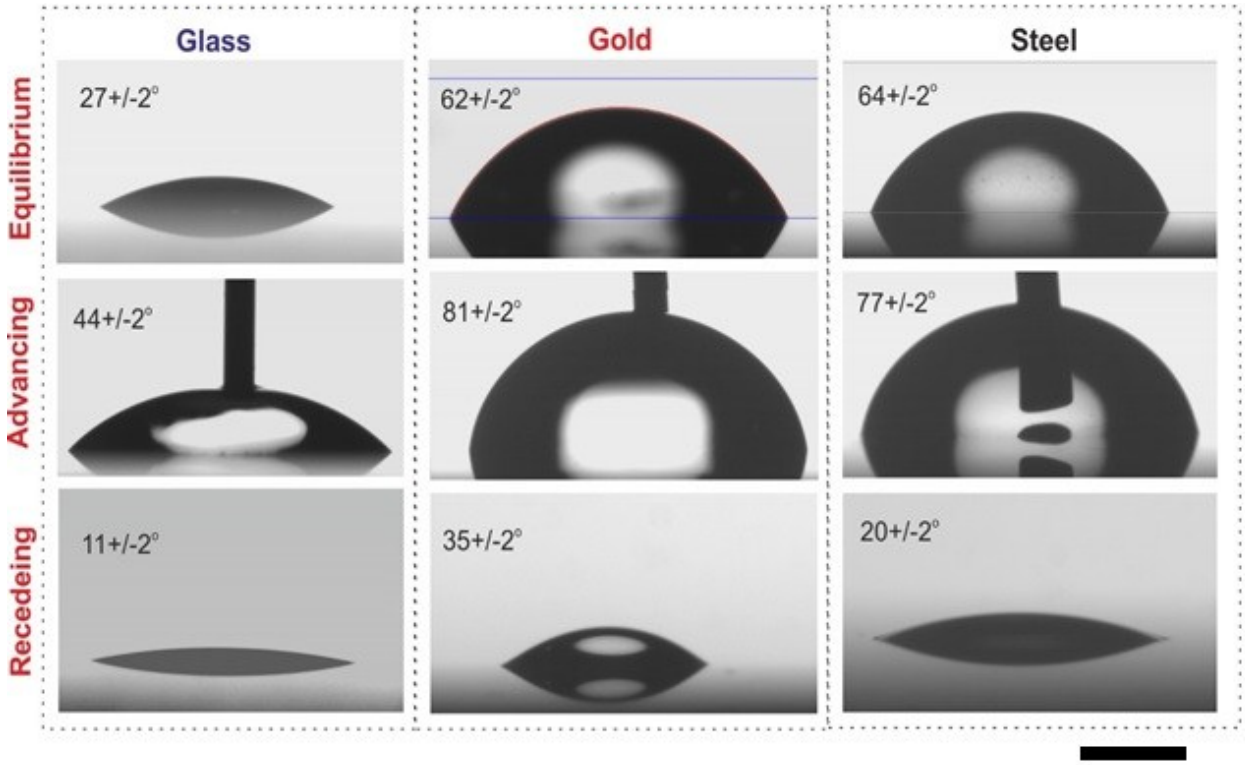

Figure S1: ***Side view images of water drops on glass, gold and steel surfaces.*** *The equilibrium, advanced and receding contact angles are shown in the panels. The receding angle was measured by letting a drop dry on the corresponding surface; the angle at which the drop-edge starts to recede was taken as the receding angle. The advancing angle was measured while infusing water into the drop though a needle. The scale bar is 1 mm.*

Hydrophobic superstrates were obtained by coating silicon surfaces with a hydrophobic silane (trichloro(1H,1H,2H,2H perfluoro-octyl) silane (Aldrich)). The process involved treating the silicon surfaces in O_2 Plasma for 2 min at 100 W, and immersing them in a solution of 30 µl of silane in 50 ml of heptane (Aldrich) for 10 min. The surfaces were washed gently in ethanol and blow-dried with nitrogen. The equilibrium and receding contact angles were 107+/3^o and 90 +/-3^o.

Preparation of solutions. Polystyrene particles (Bangs Laboratories Inc.) of diameter 0.1, 0.3, 1.0, 4.8 and 10 µm were dispersed in deionized water (or KCl solutions with concentration ranging from 0.1 mM to 1 M) at volume fractions ranging from 0.02 % to 2.5 %. The particles were washed in the corresponding solutions (deionized water or KCl) to avoid the presence of any surfactants, by centrifuging at 5000 rpm for 3 min. Similarly, silica particles of diameter 4.8 µm (Microparticle, Germany) were prepared in deionized water at volume fractions ranging from 0.05 % to 0.5 %. Blood sample was prepared by diluting with PBS (10X). Solutions of bovine serum albumin (BSA) (10 mg/ml in deionized water) containing dispersed polystyrene particles of diameter 4.8 µm were also prepared.

Experimental procedure. The IDT was placed on a Peltier element connected to an in-house PID controller to maintain the temperature at 24 ^{o}C (room temperature). The overall temperature change of the system

was separately monitored using an infrared camera (FLIR i60; FLIR systems). At higher powers (~32 dBm) the transmission of the SAW increases the temperature of the superstrate and the drop by ~4 ^{o}C.

An analogue signal generator (Agilent Technologies MXG, N5181A) was used in conjunction with a 5-500 MHz amplifier (Mini Circuits ZHL-5W-1; gain 5000) and a 3 A, 24 V DC power supply to power the IDT. The power values mentioned in the text are the power reaching at the IDT after the amplification. Unless otherwise specified, the frequency and power applied to IDT were 9.73 MHz with +/- 0.1 MHz linear sweep and 30 dBm (=1W), respectively.

The experimental setup is illustrated in Fig. 1 in the main text. The superstrate was placed overlapping about 3 mm on the edge of the IDT with about 5 µl of KY-Jelly (Johnson & Johnson) between them to provide efficient coupling. Drops of volume 2 µl were deposited on the superstrate and allowed to dry, while the SAW was applied. The drying drops were imaged through an inverted microscope (Zeiss) with a CCD camera (ProgRes, Jenoptik) in bright field or fluorescent mode.

Measuring the particle velocities. The particle movements were recorded using the inverted microscope in combination with a high speed camera (MotionScope, M2). Velocities of both the capillary flow and flow to the nodes of standing SAW were measured by tracking (ImageJ) the polystyrene particles of diameter 4.8 µm dispersed in the drop. For each data point, velocities of at least 10 particles were averaged. To obtain u_{ac} as a function of distance from the node (Fig. 4b in the main text) we considered particles moving to the nodes in a direction towards the contact line and opposite to it. The corresponding velocities are $u_{ac} + u_{evp}$ and $u_{ac} - u_{evp}$. An averaging removes the contribution of u_{evp} giving the value of u_{ac}, since any variation in u_{evp} over a distance $\lambda_{PW}/2$ from a node can be neglected.

Vibrometer measurements. The surface vibrations of the IDT and the superstrate were characterized by a vibrometer (Polytech UHF-120). The vibrations of the superstrates were measured at different individual frequencies and while the frequency sweep was applied. In all cases, we confirmed the presence of the standing waves on the surface.

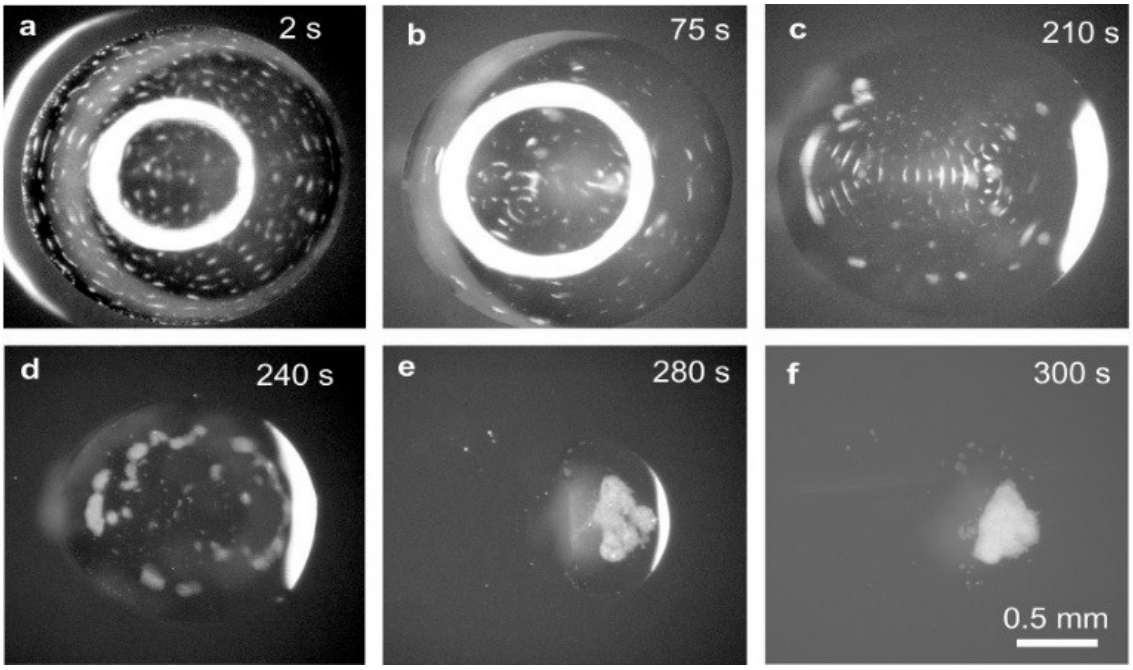

Figure S2: ***Bright field images of an evaporating drop containing silica particles (with SAW ON)****. The thick white circles in (a) and (b) and shades in (c-e) are the reflection of light. The silica particles stay close to the solid surface and away from the liquid-air interface. Therefore, they are trapped in the nodes of the acoustic pressure waves (a-d). The separation between the nodes stays as* $\lambda_{PW}/2$*. When the liquid-air interface approaches the solid surface (by approximately 80 % of the total evaporation time) particles are also trapped in the nodal circle of the standing capillary wave near the drop edge as manifested by the thick circular accumulation in (c) and more clearly in (d). Particles are concentrated at a spot even before the completion of the evaporation process (e). Upon drying, a concentrated spot of residue is formed (f). Initially, the drop (of volume 1 µl) contained silica particles of diameter 4.8 µm at a volume fraction of 0.2 %.*

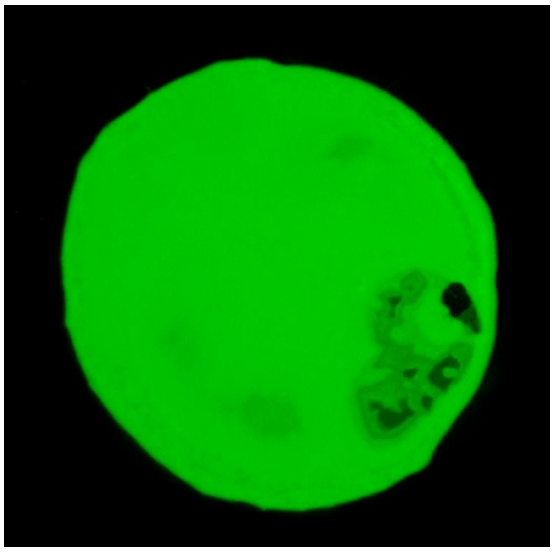

Figure S3: ***Residue at volume fraction 2.5% and frequency 9.7 MHz****. At lower frequencies the residue was disc-like, however, with regions of low particle density. At higher frequencies the residue becomes more uniform (Fig. 1d in the main article) because the nodal regions are more closely spaced. The particles were of polystyrene.*

Different superstrate materials

Besides glass, we used two other hydrophilic surfaces namely gold and steel, which are commonly used for drying drops for analytical applications [3, 4, 5, 6], and achieved successful suppression of the coffee ring effect (see Fig.S4). The equilibrium contact angles (receding angle) for water were 62+/-2^{o} (35+/-2°) and 64+/-2^{o} (20+/-2°) for gold and steel surfaces, respectively.

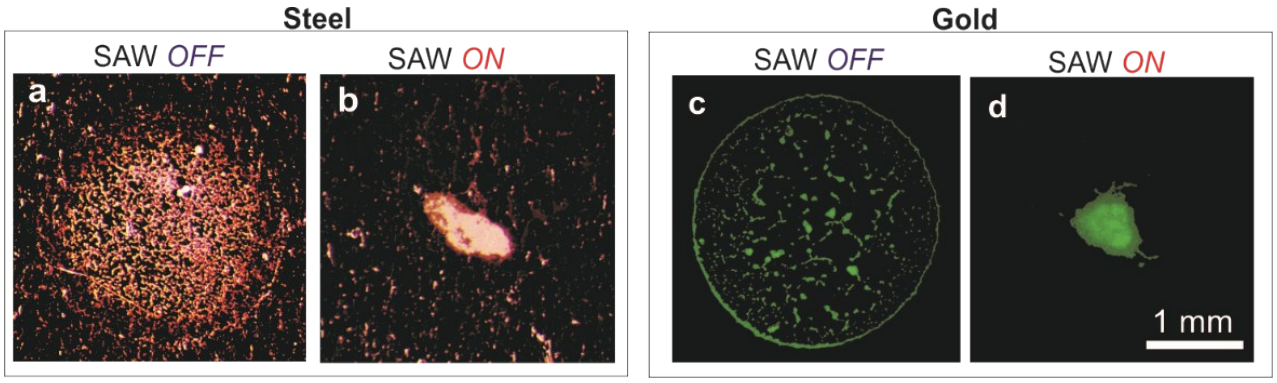

Figure S4: ***Residues on metallic surface****. (a, b) Bright field images of residues on steel surface. (c, d) Fluorescent images of residues on gold surface. The drop contained polystyrene particles of diameter 4.8 µm with an initial volume fraction of 0.05 %. SAW OFF and SAW ON represent drying undisturbed and with the application of the SAW, respectively.*

Hydrophobic surfaces are commonly used for alleviating the coffee-ring effect. When drying our BSA solution containing 4.8 µm polystyrene particles on hydrophobic surfaces, we obtained large heterogeneous residues. When applying SAW, however, the drops yielded spot-like residues (Fig. S5). Even without adsorbing components (i.e. only polystyrene particles in water), the coffee ring effect was only partially suppressed on hydrophobic surfaces, producing small ring-like residues. In such cases, our technique can totally suppress the effect to form tight spot of residues.

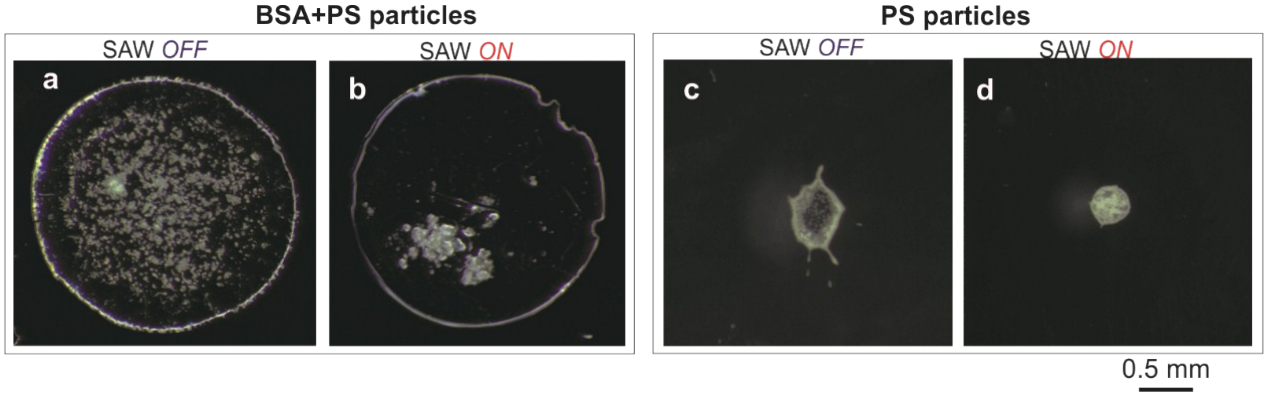

Figure S5: ***Residues on hydrophobic surface.*** *Bright field images of residues of drops containing (a,b) BSA and polystyrene particles of diameter 4.8 µm with a volume fraction of 0.05 % and (c,d) without BSA. Although the surface was hydrophobic (having equilibrium and receding contact angles for water 107+/3º and 90 +/-3º, respectively), in the case of undisturbed drying, a large residue was formed when adsorbing components (BSA) were present in the liquid, and (c) a small ring-like residue was formed without any BSA. In both cases, when the SAW was applied a concentrated spot-like residue was obtained. The initial drop volume was 2 µl.*

Since our technique relies upon keeping the contact line free of particles to facilitate its receding, the receding angle must be >0° to achieve a successful suppression. However, even when the receding angle is 0°, i.e. when the contact line is pinned during the entire evaporation process as in the case for a glass surface treated with oxygen plasma, a partial suppression was achieved (Fig. S6). The particles were trapped and concentrated, however, at the final stage of the evaporation process, the dominating capillary flows spread the trapped particles.

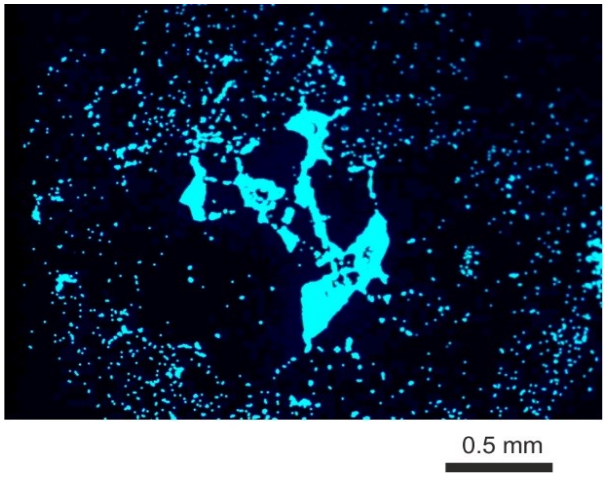

Figure S6: ***Residue on oxygen plasma treated glass.*** *In our technique, the contact line is kept free of particles to recede during the evaporation process. It means that the receding angle must be above zero degree to achieve a successful concentration of the sample. When the glass surface was treated with oxygen plasma (for 10 s at 50 W power), the receding contact angle became zero degree, i.e. the contact line was pinned during the entire drying process. When the SAW was applied, the particles were still trapped and then concentrated, however at the final stage, the dominating capillary flows spread the trapped particles. The drop contained polystyrene particles of diameter 4.8 µm with an initial volume fraction of 0.05 %. The equilibrium contact angle on the surface was 12 +/-2 degrees.*

Different solutions

We also demonstrated the suppression of the coffee ring effect on glass with diluted (10X in PBS) blood samples, where the particles of interest are the blood cells and with a solution of BSA (10 mg/ml in deionized water) containing dispersed polystyrene particles of diameter 4.8 µm (Fig. S7). As the drop evaporated the contact line receded in a stick-slip manner. Since abundant proteins cannot be trapped acoustically they formed a pancake-like residue with a thick edge in both cases. However, the particles in the solutions were concentrated at a spot.

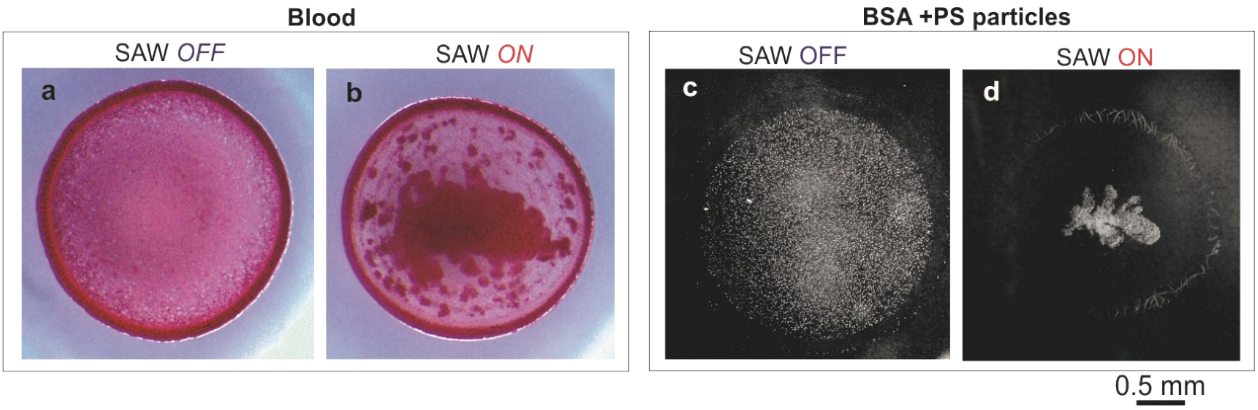

Figure S7: ***Drying bio samples on glass surface****. Bright field images of the residues of: (a, b) blood diluted 10 times in PBS, (c, d) polystyrene particles of diameter 4.8 µm dispersed in BSA. SAW OFF and SAW ON represent drying undisturbed and with the application of the SAW, respectively. Although, the abundant protein molecules in the solution form thick edges in (d) the contained particles can be concentrated.*

Effect of streaming flows

Streaming flows can prevent trapping of small particles; but at the same time, it disturbs the evaporation-driven transport of particles to the contact line. We observed that the streaming effects, although weak in our system, existed mainly at the central region of the droplet, and therefore, near the contact line the evaporation-driven flow velocity, u_{evp} was dominated. As a result, in our system, streaming did not alter the condition $^{u_{ac,mx}}> u_{evp}$ for a successful suppression.

Supplementary movies

Movie 1

Evaporation of a drop with polystyrene particles. The drop of volume 2µl contained 4.8 µm polystyrene particles at volume fraction 0.5%. The superstrate surface was glass. The SAW was applied at a frequency of 9.7 MHz with a frequency modulation by 0.2 MHz (with a modulation interval of 2 s). The particles are accumulated along the nodal circles dictated by the capillary waves. As the evaporation proceeds, the distance between the adjacent nodal circles increases and the number of nodal circles decreases. In real time, the drop took about 500 s for drying.

Movie 2

Evaporation of a drop with silica particles. The drop of volume 1µl contained 4.8 µm silica particles at volume fraction 0.2%. The superstrate surface was glass. The SAW was applied at a frequency of 9.7 MHz with a frequency modulation by 0.2 MHz (with a modulation interval of 2 s). The particles stayed close to the solid-liquid interface. Therefore, they accumulated along the nodal regions dictated by the

acoustic pressure waves and least affected by the capillary waves at the liquid-air interface. The separation between the adjacent nodal regions stayed at $\lambda_{PW}/2$ throughout the evaporation process. In real time, the drop took about 300 s for drying.

References

1. R. Wilson, J. Reboud, Y. Bourquin, S. L. Neale, Y. Zhang, and J. M. Cooper*, Lab Chip,* 2011, **11**, 323.

2. J. Reboud, R. Wilson, Y. Zhang, M. H. Ismail, Y. Bourquin, and J. M. Cooper, *Lab Chip, 2012,* **12**, 1268.
3. A. N. Rao, and D. W. Grainger, *Biomater. Sci*., 2014, **2**, 436.
4. Y. Kim, G. B. Hurst, M. J. Doktycz, and M. V. Buchanan, *Anal. Chem.*, 2001, **73**, 2617.
5. S. Weidner, P. Knappe, and U. Panne, *Anal. Bioanal. Chem.*, 2011, **401**, 127.
6. J. B. Hu, Y. C. Chen, and P. L. Urban, *Anal. Chim. Acta* 2013, **766**, 77.